Zirconia ZrO_2 Films on Si (100) Made by Ion-Beam Sputtering Deposition: Structure and the Interfacial Layer Growth Dynamics

V.Sh. Aliev, V.V. Atuchin*, V.N. Kruchinin**, L.D. Pokrovsky*, and C.V. Ramana***

Institute of Semiconductor Physics SB RAS, Novosibirsk, 630090, Russia
Phone: +8(383) 330-69-44, Fax: +8(383) 333-27-71, E-mail: aliev@thermo.isp.nsc.ru
**Institute of Semiconductor Physics SB RAS, Novosibirsk, 630090, Russia*
***Institute of Catalysis SB RAS, Novosibirsk, 630090, Russia*
****University of Texas at EI Paso, EI Paso, Texas 79968, USA*

Abstract – Zirconia ZrO_2 is considered as a promising dielectric to replace SiO_2 in advanced metal oxide semiconductor devices in gate stack. In this article ZrO_2 films were prepared on Si (100) by method of ion-beam sputtering deposition. RHEED, HRTEM and spectral ellipsometry were used to study ZrO_2–Si interface layer and thermal stability of ZrO_2 films. It was revealed that a 2 nm thick interfacial layer (IL) is formed at ZrO_2–Si interface for the as-grown ZrO_2. Annealing at 600–900 °C results in growth of IL and crystallization of ZrO_2. Analysis of ellipsometry data showed the dispersion of refractive index for the IL, which matches with that of amorphous SiO_2. The IL growth at 900 °C, as a function of annealing time, exhibited a two step behavior with a slow and a fast growth-rate zones. The slow-rate growth of IL is due to oxygen transport in amorphous ZrO_2. The faster-rate growth is attributed to the transition from disordered to ordered state of ZrO_2. Crystallization and grain boundary formation in ZrO_2 enhance oxygen diffusion through the layer to the Si substrate. We conclude that thermally induced structural modification of the ZrO_2 film from amorphous to crystalline state causes the transition from slow to fast interfacial oxidation.

1. Introduction

Zirconia (ZrO_2) is an important material with a potential for a wide range of technological applications: electronics, magnetoelectronics, and optoelectronics [1–7]. Most importantly, ZrO_2 is considered as a promising dielectric to replace SiO_2 in advanced metal oxide semiconductor devices in gate stack [4–6]. However, it is well known that the electrical and optical properties of ZrO_2 thin films are highly dependent on the film-substrate interface structure, morphology, and chemistry, which are in turn controlled by the filmfabrication technique and postdeposition processes [1–8].

The chemical reaction between ZrO_2 and Si substrate during fabrication or postdeposition annealing process resulting in the formation of interfacial layer (IL), with silicon oxide (SiO_2), or metallic Zr clusters, or Zr-silicate ($ZrSi_xO_y$), or a combination of these, has been found in most of the earlier investigations, although the proposed mechanism varies greatly [3–6, 8]. Interfacial chemical compounds from the interfacial reaction suppress the effective dielectric constant and degrade the device performances. As such, elucidation of the ultramicrostructure, and electronic properties of ZrO_2 films has recently been the subject of numerous investigations. However, the existing data and reports on the IL growth dynamics at postdeposition process are meager. In this context, the present investigation has been performed to understand the IL growth dynamics at postdeposition annealing of ZrO_2 films grown on *n*-type Si(100) substrates using ion-beam assisted sputter deposition.

2. Experiment

Spectroscopic ellipsometry (SE) [9, 10] has been employed in combination with the reflection high energy electron diffraction (RHEED) and high-resolution transmission electron microscopy (HRTEM) to study the optical properties and thermal stability of the ZrO_2^- Si system. The ZrO_2 films were deposited on *n*-type singlecrystalline Si(100) substrates using an ARC-12M sputtering device using Zr metal as a target. The Si substrate was subjected to chemical cleaning procedure and treatment in diluted HF to remove the native oxide layer on the surface. An argon (Ar)/oxygen (O_2) mixture was introduced into the vacuum chamber, which was initially pumped down to a pressure of 10^{-6} Torr, during film deposition. The pressure in the chamber was kept at 10^{-3} Torr during deposition, and the films were made at a low substrate temperature T_S of 70 °C. TEM measurements were performed on the crosssectional ZrO_2^-/Si specimens using a JEOL JEM2010F at an accelerating voltage of 200 kV. RHEED measurements were performed using an EFZ4 device (Carl Zeiss) on the as-grown and finally annealed ZrO_2 samples to assess their surface structure. The technical details of HRTEM, RHEED and cross-sectional sample preparation procedures are described elsewhere [11, 12]. SE measurements were made on ZrO_2 films using a Spectroscan ellipsometer in the spectral range of 250 ÷ 900 nm at an incidence angle of 70°. Annealing of the ZrO_2^-/Si samples was performed in air using

a conventional furnace. Two sets of annealing experiments were performed: a) in the temperature range of 600–900 °C at a constant annealing time of 1 h and b) high-temperature annealing at 900 °C as a function of annealing time.

3. Results and discussion

The RHEED analysis indicates the amorphous nature of as-grown ZrO_2 films. The HRTEM micrograph of the ZrO_2/Si cross-sectional structure is shown in Fig. 1. The existence of an IL between the ZrO_2 and Si is evident in the HRTEM image, which indicates that the reaction between the Si substrate and growing ZrO_2 film readily takes place even without a high-T_S. HRTEM results indicate the amorphous nature of the IL, which is about 2 nm thick (Fig. 1).

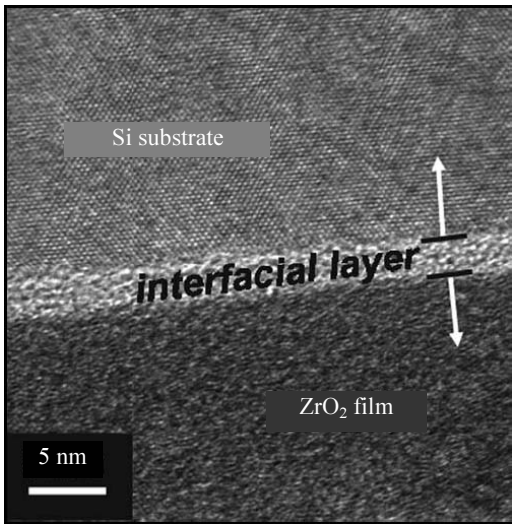

Fig. 1. HRTEM image of ZrO_2 films grown on Si(100) substrate

The chemical analyses (not shown) indicate that the grown ZrO_2 layers are stoichiometric with all of the Zt ions in the Zr^{4+} state [12].

Optical properties and interfacial oxide growth behavior of ZrO_2 / Si system have been primarily probed by SE, which measures the relative changes in the amplitude and phase of the linearly polarized monochromatic incident light upon oblique reflection from the film surface [9, 10]. The experimental parameters obtained by SE are the angles Ψ (azimuth) and Δ (phase change), which are related to the microstructure and optical properties, defined by

$$\rho = R_p / R_s = \tan\Psi \cdot \exp(i\Delta), \qquad (1)$$

where R_p and R_s are the complex reflection coefficients of the light polarized parallel and perpendicular to the plane of incidence, respectively. The spectral dependencies of Ψ and Δ can be fitted with appropriate models to extract the film thickness and the optical constants: the refractive index n and extinction coefficient k [10].

The spectral dependences of $n(\lambda)$ and $k(\lambda)$ calculated using a simple model for ZrO_2 films is shown in Fig. 2. The $n(\lambda)$ and $k(\lambda)$ dispersion curves are in good agreement with those reported for amorphous ZrO_2 [13]. The extinction coefficient (k) being low and very close to zero indicates very small optical loss due to absorption.

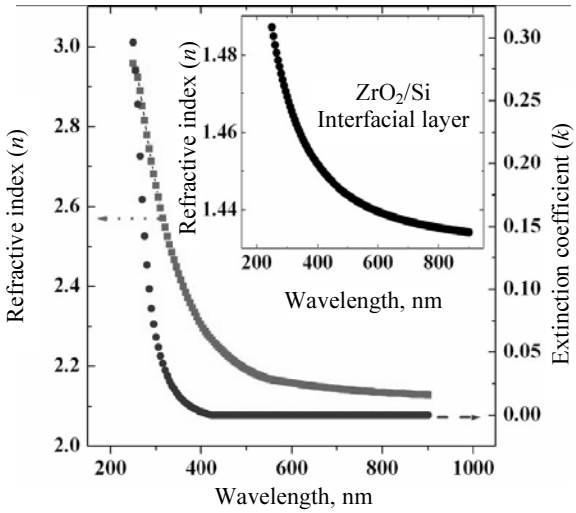

Fig. 2. The spectral dependence of the optical constants, n (o – points) and k (– points), of ZrO_2 films derived from SE data. Inset shows the dispersion of refractive index obtained for the IL

The dispersion relation of $n(\lambda)$ evaluated for the IL is shown as an inset in Fig. 2. The $n(\lambda)$ vs λ curve is very similar to that of amorphous SiO_2 [14], thus indirectly confirming the SiO_2-based chemical nature of the IL.

SE is very sensitive to the IL formation and the simple model as described for the as-grown ZrO_2 /Si structure was not suitable to fit the experimental results in the case of annealed samples. Thus, a more complicated two-layer model is adopted. The system consists of an array (air)/(first isotropic homogeneous layer with thickness $L1$)/(second isotropic homogeneous layer with thickness $L2$)/(Si substrate), whereby thicknesses $L1$ and $L2$ are varied during fitting. The values of $L1$ and $L2$ are presented in Fig. 3 along with the representation of the model adopted.

The data are presented as a function of the square root of the annealing time to indicate the two-step behavior of the thermal oxidation process noticed in the present work. A continuous increase in $L2$ adjacent to Si substrate with annealing time is due to the oxidation of the Si substrate by oxygen diffused from air through the ZrO_2 layer. Thus, this IL, which is $L2$ in SE model notations, is mostly SiO_2 in chemical composition, but possible Zr-doping cannot be excluded. The growth rate of IL is controlled by three elemental stages, namely, adsorption of oxygen on the top surface of ZrO_2, diffusion through the ZrO_2 layer, and diffusion through the SiO_2 layer to the oxidation front at the interface SiO_2 /Si.

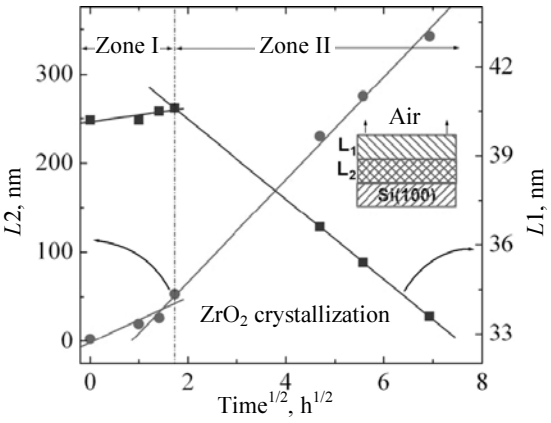

Fig. 3. Growth dynamics of the thicknesses $L1$ (– points) and $L2$ (o – points) obtained on the ZrO_2 layers and interfacial SiO_2 layer as a function of time of annealing at 900 °C

A model can be formulated to explain the observed IL growth dynamics at postdeposition annealing of the ZrO_2/Si system. The as-deposited ZrO_2 layer is completely amorphous as confirmed by RHEED and HRTEM observations. The IL thickness increases, with the time of annealing, which is due to the oxidation of the ZrO_2/Si interface. Oxygen needed for this process is provided by the interaction of the topmost surface layers with air at high temperature. Subsequently, the diffusion of oxygen through ZrO_2 layer causes further oxidation of the Si substrate layers into SiO_2. The interesting point is that the IL oxide growth as a function of annealing time shows a two-step behavior (Fig. 3) with a clear distinction of two regions, which are labeled zone I and zone II. The growth rate is rather slow in zone I, where the oxygen transport is, perhaps, controlled by a slow-diffusion process through the relatively thick amorphous ZrO_2 layer at the surface. Continued annealing for more than 3 h shows a transition of the oxidation behavior into zone II, where the growth rate of the IL is fast. A slight decrease in thickness of the ZrO_2 layer is noticed corresponding to the fast-rate zone II. This observation indicates the crystallization of the amorphous ZrO_2 layer with increasing annealing time.

Crystallization of amorphous ZrO_2 results in a drastic shrinkage of the film volume because of intensive crystal grain formation with dense atomic packing and structural ordering. As a result, the interstitial diffusion mechanism of oxygen in ZrO_2 becomes less important and oxygen transport is mainly taken over by high-rate crystal grain boundary diffusion that facilitates the faster oxygen transportation to SiO_2/Si interface. Therefore, crystallization of ZrO_2 with formation of grain boundaries is mainly responsible for initiating zone II stage of the oxidation process. Crystallization of ZrO_2 at 700–900 °C as reported in earlier studies [8] and confirmed by the RHEED pattern in the present work provides evidence that the change in oxidation behavior is due to a transition from a disordered to ordered state. Furthermore, Busch *et al.* reported the fast interfacial oxidation at the ZrO_2/Si based on oxygen diffusion at the crystalline boundary [15]. A higher oxygen diffusivity (10^3–10^4 times faster) was also reported for polycrystalline ZrO_2 than that in the bulk crystal. We, therefore, conclude that thermally induced structural modification of the ZrO_2 film from amorphous to crystalline state causes the transition from slow to fast interfacial oxidation zone [16].

References

[1] D. Chi and P.C. Mclntyre, Appl. Phys. Lett. **88**, 232901 (2006).
[2] C.M. Wang, S. Azad, S. Thevuthasan, V. Shutthanandan, D.E. McCready, and C.H.F. Peden, J. Mater. Res. **19**, 1315 (2004).
[3] S. Venkataraj, O. Kappertz, R. Jayavel, and M. Wuttig, J. Appl. Phys. **92**, 2461 (2002).
[4] D. Chi and P.C. Mclntyre, Appl. Phys. Lett. **85**, 4699 (2004).
[5] J. Robertson, Solid-State Electron **49**, 283 (2005).
[6] C.M. Lopez, N.A. Suvorova, E.A. Irene, A.A. Suvorova, and M. Saunders, J. Appl. Phys. **98**, 033506 (2005).
[7] S. Honda, F.A. Modine, A. Meldrum, J.D. Budai, T.E. Haynes, and L.A. Boatner, Appl. Phys. Lett. **77**, 711 (2000).
[8] L.M. Chen, Y.S. Lai, and J.S. Chen, Thin Solid Films **515**, 3724 (2007).
[9] H. Fujiwara, *Spectroscopic Ellipsometry: Principles and Applications*, New York, Wiley, 2007, p. 81.
[10] G. E. Jellison, Jr., Thin Solid Films **13**, 33 (1998).
[11] C.V. Ramana, A. Ait-Salah, S. Utsunomiya, U. Becker, A. Mauger, F. Gendron, and C.M. Julien, Chem. Mater. **18**, 3788 (2006).
[12] C.V. Ramana, V.V. Atuchin, U. Becker, R.C. Ewing, I.L. Isaenko, O.-Yu. Khyzhun, A.A. Merkulov, L.D. Pokrovsky, A.K. Sinelnichenko, and S.A. Zhurkov, J. Phys. Chem. C. **111**, 2702 (2007).
[13] A. R. Farouhi and I. Bloomer, Phys. Rev. B **34**, 7018 (1986).
[14] G.L. Tan, M.F. Lemon, D.J. Jones, and R.H. French, Phys. Rev. B **72**, 205117 (2005).
[15] B.W. Busch, W.H. Schulte, E. Garfunkel, T. Gustafsson, W. Qi, R. Nieh, and J. Lee, Phys. Rev. B **62**, R13290 (2000).
[16] U. Brossmann, R. Wurschum, U. Sodervall, and H.-E. Schaefer, J. Appl. Phys. **85**, 7646 (1999).